Biotechnology Reports 7 (2015) 95–106

Contents lists available at ScienceDirect

Biotechnology Reports

journal homepage: www.elsevier.com/locate/btre

Rice husk extracted lignin–TEOS biocomposites: Effects of acetylation and silane surface treatments for application in nickel removal☆

Kumari Shweta, Harit Jha*

Department of Biotechnology, Guru Ghasidas Vishwavidyalaya (A Central University), Bilaspur 49500, Chhattisgarh, India

ARTICLE INFO

Article history:
Received 27 October 2014
Received in revised form 6 May 2015
Accepted 10 May 2015
Available online 11 June 2015

Keywords:
Rice husk (RH)
Lignin–TEOS biocomposites
Sol–gel chemistry
Differential scanning calorimetry (DSC)
Metal removal
FTIR

ABSTRACT

A novel lignosilicate (LS) composite was synthesized from pre-extracted (hot water, 80% ethanol, 0.3 N NaOH) lignin of rice husk (RH) using TEOS as matrix. The extracted lignins were subjected to surface modification by acetylation followed by in situ synthesis of lignosilicate (LS) composites by sol–gel method for application in nickel removal. LS were characterized by FT-IR, scanning electron microscopy (SEM), differential scanning calorimetry (DSC), particle size distribution (PSD) and atomic absorption spectroscopy (AAS). FT-IR studies showed acetyl group in the range of 1680–1690 cm^{-1} whereas for adsorbed Si—O—Ni^{2+} the band appeared at 870 cm^{-1}. Findings suggest that alkali extracted LS with mean PSD of 14.89 nm are thermally more stable (T_m = 337 °C) than ethanol (ELS) and hot water (HLS) extracted LS, and exhibit potential for Ni^{2+} removal (38.74%). SEM and PSD (D_{50}) analyses confirmed their rough surfaces and dispersive nature, respectively, suitable for metal biosorption.

1. Introduction

Agricultural wastes directly affect our natural resources. They cause ecological problems due to their low natural degradation rate and consequent elimination by burning, thus they are major source of atmospheric pollution. It is, therefore, very important to develop new and safe methods to utilize agrowastes and to overcome environmental problems. Cell walls of agrowastes are composed of cellulose, hemicellulose and lignin. Among these lignin is the second most abundant natural biopolymer of plant biomass [1]. It has a complex chemical structure and is chemically and physically heterogeneous in nature. Lignin may be an important bioresource for synthesis of value added products and their subsequent applications. Presence of significant amounts of different oxygen-containing groups in lignin allows physical adsorption, hydrogen bonding, coordination and covalent linking as well as acidic–basic interaction with other compounds [2–5]. In order to improve the reactivity of lignin, many methods have been proposed, including methylation, demethylation, acetylation, etc. To modify the pore structures of the natural biopolymer, it may be fixed within the silica xerogel matrix through hydrolysis and condensation reactions [6].

Organic–inorganic composites are the new class of high performance and highly functional materials [7,8]. Naturally occurring organic polymers have been combined with silica by the sol–gel method to achieve various silica–organic hybrids [4,5]. They are cheap and easily processed nevertheless prolonged exposure to UV light and some solvents cause the degradation of polymer. Inorganic compounds generally have high chemical and thermal stability that allow their applications under different operating conditions. Organic compounds are characterized by synthetic versatility and reactivity, thus making it possible to modulate the molecular structure of the sensing materials and enhance the selectivity toward a target component [9–11]. The variability and site recognition of biopolymers, such as lignocelluloses, DNA and other carbohydrates offer a wide range of opportunities for the self-organization/assembly through weak interactions, such as H-bonds, hydrophobic, or van der Waal interactions (generally in aqueous environments) and hence require quite different synthetic strategies.

The sol–gel technique is a long established industrial process for the generation of colloidal nanoparticles from liquid phase. This mechanism is well adapted for oxide nanoparticles and composite powder synthesis [7]. The main advantages of sol–gel techniques for the preparation of such materials are low temperature of processing, versatility, and flexible rheology allowing easy shaping and embedding. The commonly used precursors of oxides are known as alkoxides, mainly due to their commercial availability

* Corresponding author. Tel.: +91 9826 630805/7522 260405; fax: +91 7752 260148.
E-mail address: harit74@yahoo.co.in (H. Jha).

http://dx.doi.org/10.1016/j.btre.2015.05.003

and high liability to M—OR bond allowing facile tailoring in situ during processing [10–13].

Modified silica xerogel using lignin as an additive has already been prepared [11,15]. However, except a few reports [14,15], no serious attempt has so far been made to investigate the use of rice husk (RH) as the source of lignin to combine with silica for the production of composites by the sol–gel process. As we know that the RH, one of the major agricultural by-products of the rice milling industry, is annually produced in large quantities in all rice producing countries [15,16]. However, most of it is not utilized because of its poor protein and high ash contents [15–17]. Due to the inherent structural variations in biomass lignin as well as the structural changes that might be brought out through various chemical modifications used to obtain modified lignin, this natural biopolymer bears great scope for synthesizing diverse types of lignin based hybrids having wider applications in heavy metal bioremediation [14,15,18,19]. Trace heavy metals are the major sources of environmental pollution and are mainly released as a result of the extensive mining activities and industrial applications [19–21]. It has been well documented that excess of heavy metals has several negative impacts on the flora and fauna including human beings [14]. The toxic contribution of heavy metal ions is mainly related to the chemical forms or species rather than to the total concentration of the element [21,22].

The present study reports *in-situ* syntheses of RH-based lignin–TEOS (tetraethoxy silane) composites using sol–gel process. The influence of ratio of lignin and TEOS on the synthesis as well as structure of lignin–TEOS composites (termed as Lignosilicate or LS) was also investigated. The rationale of this study was to understand the influence of different solvents on extractability of lignin from RH, the structure of chemically synthesized composites, the effect of finely dispersed silica on the composite formation with lignin, and eventually assessing nickel adsorption capacities of the hybrids. Composites were structurally and chemically characterized by using UV–vis spectroscopy, particle size analyzer (PSD), scanning electron microscopy (SEM), Fourier transform infra-red (FT-IR) spectroscopy, differential scanning calorimetry (DSC), thermo gravimetric analysis–differential thermal analysis (TGA–DTA) and atomic absorption spectroscopy (AAS).

2. Materials and methods

2.1. Chemicals and reagents

Rice husk (RH) used for extracting lignin was purchased from the local rice mills of Bilaspur, Chhattisgarh, India. The chemicals used in the experiments were of high purity, analytical grades and obtained from commercial sources, such as Fisher Scientific (Na_2SiO_3/TEOS, 99.98%, HCl, H_2SO_4, 5 M $NiCl_2{\cdot}6H_2O$), Hi-media (NaOH, 98.0%; KBr, 99.0%) and Qualigens (sodium selenite). The solvents used were from Merck, Germany. Deionized water (Millipore, USA) was used throughout the experiments.

2.2. Experimental procedure

2.2.1. Hot water extraction of lignin from RH

The hot water extraction of lignin was performed by the method of Borrega et al. [23]. Extraction was performed with RH and water in the ratio of 1:5 (w/v) at 95 °C for 3 h. The remaining solid residues were discarded after filtration. Lignin was obtained from the aqueous supernatant by drying at 60 °C overnight in oven.

2.2.2. Extraction of lignin from RH by 80% ethanol

For ethanolic extraction of lignin, 20 g of RH was mixed with 200 mL of 80% ethanol in 1:10 (w/v) ratio. The mixture was kept for continuous shaking at 150 rpm in the shaking water bath at 75 °C for 4 h followed by filtration using Whatman filter paper (pore size 1.5 μm). Lignin was finally extracted using soxhlet apparatus.

2.2.3. Extraction of lignin from RH by 0.3 N NaOH

Alkaline extraction was performed by the method described by Altwaiq et al. [24] with minor modifications. The RH was treated with aqueous solution of 0.3 N NaOH in autoclave at 121 °C for 20 min. The ratio of husk to alkali solution was kept to 1:10 (w/v). After gravity filtration, the filtrate was acidified by addition of 5 M sulphuric acid drop-wise until the pH was lowered to 5.5 for the removal of soluble hemicelluloses. The remaining hemicellulose residues were removed by precipitation after adding three volumes of absolute ethanol followed by centrifugation at 13,000 × *g* for 10 min. The supernatant obtained was concentrated up to 20–30 mL in oven at 60 °C. Alkali soluble lignin was recovered by reducing the pH up to 1.5–2.0 with addition of 5 M sulphuric acid under continuous agitation. The precipitated lignin was sedimented by centrifugation at 15,000 × *g* for 10 min. The pellet obtained was dried in hot air oven overnight at 60 °C.

2.2.4. Lignin modification through acetylation to improve solubility

The extracted lignin samples were subjected to acetylation in order to enhance their solubility. In principle, the acetylation process involves substitution of all the hydroxyl functional groups by new acetyl groups. Lignin was modified by the method of Xiao et al. [7] with minor modifications. Briefly, 100 mg of pre-modified lignin obtained by different extraction methods was treated with 100 mL of pyridine and acetic acid mixture (1:1) under shaking conditions for 24 h at room temperature. After treatment, 80 mL of ethanol was added in the reaction mixture and the precipitate was collected by rotary evaporation. Further, the precipitates were mixed with 5 mL of chloroform and 150 mL of diethyl ether. Solution was stirred vigorously for 15 min. Finally, the modified (acetylated) lignin was obtained by filtration and dried overnight at 60 °C in oven. The acetylated lignin was weighed and stored in a glass vial for further analysis.

2.2.5. Synthesis of lignin–TEOS composites

The lignin–TEOS composites were synthesized by the method of Teofil et al. [10] with minor modifications. 100 mg of each of the modified lignin hot water extracted acetylated lignin (HAL), ethanol extracted acetylated lignin (EAL), and 0.3 N NaOH extracted acetylated lignin (NAL) samples in 100 mL (1:1 w/v) of 10 mM, 5% conc. H_2SO_4 (pH 1.8). The mixture was stirred vigorously for 15 min at 250 rpm and after shaking pH was adjusted up to 2.0 with 6% TEOS. The acidified sample was again left for shaking for 15 min. Following this, the pH of the mixture was raised to 7.0 using 6% TEOS for transition of sol–gel. A polymer gel was formed within 20 min of the incubation at the room temperature (RT). The gel was dried for a week in an oven at 60 °C to obtain LS composite and used for further characterization.

2.3. Characterization of LS composites

2.3.1. Spectral study of extracted lignin

For spectral analysis, 2.5 mL of each lignin, viz. 0.3 N NL, EL and HL (0.3 N NaOH extracted lignin, 80% ethanol extracted lignin and hot water extracted lignin, respectively), sample (50 mg mL^{-1}) was added to 0.5 mL of potassium phosphate buffer (pH 6.6). The resulting solution was dissolved in ethanol and water in a ratio of 2:1, v/v. The spectrum of all lignin samples was acquired between 200 and 400 nm using UV–vis spectrophotometer (UV-1800, Shimadzu). 2-Ethoxyethanol in deionized water (2:1, v/v) was used as the reference.

The synthesized LS composites were initially crushed in a mortar-pestle, dissolved in preheated deionized water (1:2, w/v) and sonicated using ultrasonic homogenizer (Biologics Inc. 3000) at 40 W with 60% pulse rate for 30 min before spectral analyses.

2.3.2. Particle size analysis

Particle size analyses of the synthesized LS composites were obtained using particle size analyzer (Sald-2201, Shimadzu). Before analysis samples were dissolved in preheated deionized water (1:2, w/v) and sonicated at 40 W with 60% pulse rate for 30 min, as per standard operating procedure.

2.3.3. SEM analysis of LS composites

In order to elucidate the morphology and microstructure of the LS composites electron microscopic analysis was performed using SEM (JEOL JSM—6360) at 20 kV by the method as described in the instruction manual.

2.3.4. Thermal behavior of LS hybrids

Thermo-gravimetric analysis (TGA) was carried out in the TGA instrument (PerkinElmer) to determine the maximum temperature of dehydration of solid state LS composites with degradation in terms of weight loss. Approximately, 5–10 mg sample was placed in the sample holder of the instrument and heated from 40 °C to 870 °C at a constant heating rate of 10 °C min^{-1}. The test was performed in an atmospheric nitrogen purge injected at a flow rate of 100 mL min^{-1}.

For determination of the glass transition (T_g) temperature, 6.5 mg of each sample was precisely weighed and encapsulated in an aluminum (Al) pan. The pan was then placed in a DSC instrument (DSC-60, TA-60 WS, and Shimadzu, Japan) and heated from 25 °C to 200 °C at the heating rate of 10 °C min^{-1}. The test was performed in an atmospheric nitrogen purge, injected at a flow rate of 10 mL min^{-1} using alumina (Al_2O_3) as internal standard.

2.3.5. Fourier transform infra-red (FTIR) spectroscopic analysis

Extracted and dried lignins (as control), LS composite samples were mixed with KBr at a concentration of 1 mg/100 mg KBr (w/w) for characterization by FTIR analysis. The spectra were taken in absorption mode in the range of 400–4000 cm^{-1} with 32 scans in FTIR spectrophotometer (Shimadzu 8400S, Japan) as described earlier [4].

2.4. Bio-sorption study of Ni^{2+}

2.4.1. Effect of LS composite dose on Ni^{2+} bio-sorption

The effect of two different doses of LS (0.1, 0.25, 0.5, 1.0, 1.5 and 2.0 g L^{-1}) was studied to determine the bio sorption of metal via batch equilibrium. 15 mL sample of 0.1 M and 0.2 M metal solution was then added to the selected mass of composite bio sorbent at pH 6.0. The mixture was allowed to pass through a column prepared in the 20 mL sterile dispo-van syringe (size 80 × 38 mm). The unbound metal ion was filtered, washed with 50 mL double distilled water and the metal ion concentration was determined by AAS analysis (AAS, Shimadzu, Japan).

2.4.2. Determination of Ni^{2+} biosorption by AAS analysis

Batch equilibrium process was used to determine the effect of initial concentrations of metal solution on the bio-sorption capacity. As described in the previous section two different concentrations of metal at pH 6.0 (adjusted with 0.1 N HCl) were prepared to cover a wide range. 15 mL of metal solution was subsequently added to different doses of samples of the bio-sorbent. Rest of the procedure was completed as described previously [19].

Total dissolved metal was determined by AAS analysis after acid digestion of metal solutions in a mixture of HNO_3:HCl, 3:1 v/v (aqua-regia). Eluted test samples of metal were mixed in 1:1 ratio of aqua-regia and metal solutions. Samples were kept under vigorous shaking condition for 24 h at room temperature followed by filtration (Whatman filter paper grade: 42) with retention capacity of 1.5 μm and a filtration rate at 4 mL min^{-1}). Filtrates were collected in a glass vial. The residual LS composite (acting as an adsorbent) was used for analysis by FTIR to determine the bonding pattern of metal to the surface of LS composite as bio-sorbent [21].

The concentration of heavy metal ions in the aqueous solutions before (C_o) and after adsorption (C_e) was determined using AAS (AAS, Shimadzu, Japan). The amount of metal ions present in solution after adsorption (q) as per Eq. (1) and percent removal as per Eq. (2) was calculated as follows [21,22]:

$$q = \frac{(C_o - C_e)v}{w}$$

$$\%R = \frac{(C_o - C_e)}{C_o} \times 100$$

where, q (mg g^{-1}) = amount (mg) of metal ions adsorbed per gram of adsorbent (adsorption capacity):

C_o (g L^{-1}) = initial concentration of metal ions;

C_e (g L^{-1}) = final concentration of metal ions;

v (mL) = volume of metal solution;

w (g) = weight of adsorbent.

3. Results and discussion

3.1. Acetylation of lignin for ligno-silicate preparation

The yield of lignin extracted from RH by three different extraction methods was calculated. The highest yield was obtained with 0.3 N NL (20.1 ± 0.11%), followed by EL (6.86 ± 0.14%) and HL (14.95 ± 0.12%). The three solvent extracted lignin samples were modified by acetylation reaction to obtain free functional groups [25]. The highest yield was obtained as ethanolic acetylated lignin (EAL, 16.71 ± 0.02%) whereas other lignin fractions showed lower yields; 13.67 ± 0.01% as 0.3 N NaOH acetylated lignin (0.3 N NAL) and 11.19 ± 0.01% as hot water acetylated lignin (HAL).

Higher percentage of yield could be achieved only if the reactivity of the extracted lignin gets chemically enhanced and one of the most reactivity-enhancing processes used in our study was acetylation for hybrid synthesis as described by Atwood and Lehn [8]. Previous reports suggested that the lignin yield was dependent on the solvent used; the concentration of alkali might efficiently reduce the complexity and molecular size of acetylated lignin and disrupt the chemical bonds present in lignin, cellulose and hemicelluloses [2,26]. The solvents primarily act by promoting the impregnation of vegetal tissue leading to solubilization of lignin fragments. The carbonium ions in the resulting intermediates react with an electron-rich carbon to form stable carbon–carbon linkages, leading to condensation of lignin [27,28]. Ethanol extraction, therefore, is one of the most important procedures for the structural characterization or modification of polymer of ligno-cellulosic materials [28].

3.2. UV–vis spectra

The absorption spectra of acetylated lignin samples were measured in the range of 200–600 nm. The maximum absorbance (λ_{max}) of HAL, EAL and 0.3 N NAL were found at 290 nm, 280 nm

and 320 nm, respectively. The highest absorbance value (λ_{max}) was shown by 0.3 N NAL due to the conjugated structures of acetyl group and α-carbonyl groups [29].

The λ_{max} of hot water ligno silicate (HLS), 80% ethanolic ligno silicate (ELS), 0.3 N NaOH ligno silicate (0.3 N NLS) and TEOS were obtained at 420 nm, 350 nm undefined, 420 nm and 415 nm, respectively (Fig. 1a and b). A high intense peak at 480 nm was observed in HLS and 0.3 N NLS (Fig. 1a and b). This peak appeared mainly due to the electronic transition of non-conjugated aromatic ring as described earlier [28–30].

3.3. Characterization of ligno-silicate composites

3.3.1. FTIR spectrum of RH extracted lignin and LS composites

Fig. 2(a) shows the comparative FTIR spectra of organosolv lignin (0.3 N NAL) with solvent treated (80% ethanol) and hot water extracted lignin. The absorption bands appeared at 1600, 1520, 1440, 1100, 1000 and 800 cm^{-1} corresponding to C=C aromatic ring stretching, C—C aromatic skeletal vibration, aromatic ring partial double band of C—C symmetric vibration, C—H in plane deformation, stretch vibration for C=O of alcohol and aromatic C—H out of plane determination. The bands for impurity appeared at 1049 cm^{-1} and 1220 cm^{-1}, confirmed the presence of hemicelluloses in small amount in the organosolv lignin samples [31].

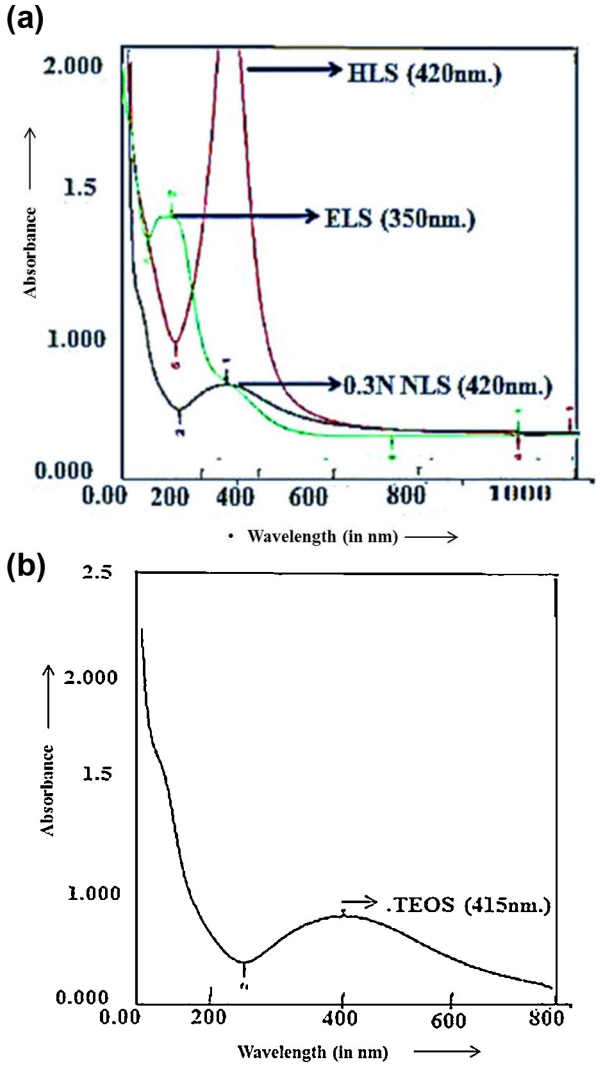

Fig. 1. (a) UV–vis spectrum of lignin–TEOS composites and (b) UV–vis spectrum of TEOS.

An absorption band at 1220 cm^{-1} corresponding to syringyl unit was observed in almost all organosolv lignin samples. The occurrence of syringyl unit in hardwood lignin was also marked by a band at 1462 cm^{-1} [32] in all the samples analysed. FTIR absorption bands at 3400 cm^{-1} might be attributed to O—H stretching of aromatic ring or aliphatic chains. Bands at 2917.14, 2918.1 and 2896.76 cm^{-1} were related to the C—H vibration of CH_2 and CH_3 groups of the aromatic ring.

Comparative FTIR band spectra are shown in Fig. 2(a). Acidic lignin bands were found at 1720, 1600, 1520, 1412, 1100, and 800 cm^{-1} corresponding to C=O stretch in unconjugated carboxyl group, C=C aromatic ring stretching, C—C aromatic skeletal vibration, partial double band of C—C symmetric vibration, C—H in plane deformation determined of S unit and aromatic C—H out of plane determination, respectively. Absorption bands of samples confirmed the existence of phenolic aromatic contents in the sample. The peak of C=O stretch of carboxylic group was illustrated. It might have been originated due to the characteristic of the carboxylic group which did not lose at the time of extraction. The peak at 1037 cm^{-1} was originated possibly due to the small amount of hemicelluloses impurities in the treated husk.

The spectra of hot water extracted samples shown all characteristic bands of lignin functional groups at fingerprint region along with a band of hemicellulose impurity, moisture content in the sample and carboxylic group absorption band. The analysis of FTIR spectra of all extracted lignin samples suggested that the lignin obtained through alkali extraction method was most purified with lower levels of impurities.

Lignin and silica compounds have a terminal aliphatic hydroxyl group at C-3 on the side chain besides a phenolic hydroxyl group at C-4 of the aromatic ring [2]. Chemical functionalization by silica leads to the alteration of composition, energy and charge for the attachment of functional groups of acetylated lignin during hybrid preparation through sol–gel mechanism. TEOS acts as the coupling agent for the lignin surface modification leading to synthesis of a stable hybrid even within a wide pH range. The FTIR spectra of the LS hybrids showed carbonyl stretching in acetyl group of acetylated lignin appearing in the range of 1680–1690 cm^{-1} and 1650–1660 cm^{-1} (Fig. 2b). The aromatic ring conjugated coniferyl alcohol C=C group were completely hydrogenated in the acetylated lignin as reported earlier [28].

Hydrolysis reaction of silane leads to substitution of —OH groups on the surface of lignin and the resulting Si—OH group helps in condensation reaction with organic components. Chemical hydrolysis and condensation reactions between two different phases, lead to the formation of a stable bond between two surfaces and thus releases free alcohol as a byproduct eventually resulting in the formation of lignin polyol derivatives, which in turn improves the solubility of the lignin [24,28]. The spectrum of silica revealed the presence of characteristic bonds Si—O—Si (1096 cm^{-1}, 805 cm^{-1}), Si—OH (960 cm^{-1}) and Si—O (470 cm^{-1}). The other bands showing the stretching vibration of O—H group (3600–3200 cm^{-1}) and a low-intensity one at 1643.35–1573 cm^{-1} were assigned to water physically bound to silica. Other group of bands appeared at 1454.33 cm^{-1} and 1336.67 cm^{-1} showing O—CH_3 deformation in ELS, 0.3 N NLS and HLS. Spectra at 1392 cm^{-1} showing O—H band and at 1363 cm^{-1} having C—H bends in Si—C—H bands were also obtained during investigation.

An aliphatic O—H band appeared between 1334 and 1331 cm^{-1} in 0.3 N NLS. The spectrum also showed a group of bands below 1000 cm^{-1} (997.20 cm^{-1}, 928 cm^{-1} and 619.15 cm^{-1}) which could be assigned to the in-plane and out-of-plane vibrations of aromatic C—H, C=C—H and —HC=CH— bonds in HLS and 0.3 N NLS (Fig. 2b) similar to those reported earlier [28]. An increase in the intensity of the bands could be assigned to the appropriate functional groups compared to the unmodified silica spectrum and

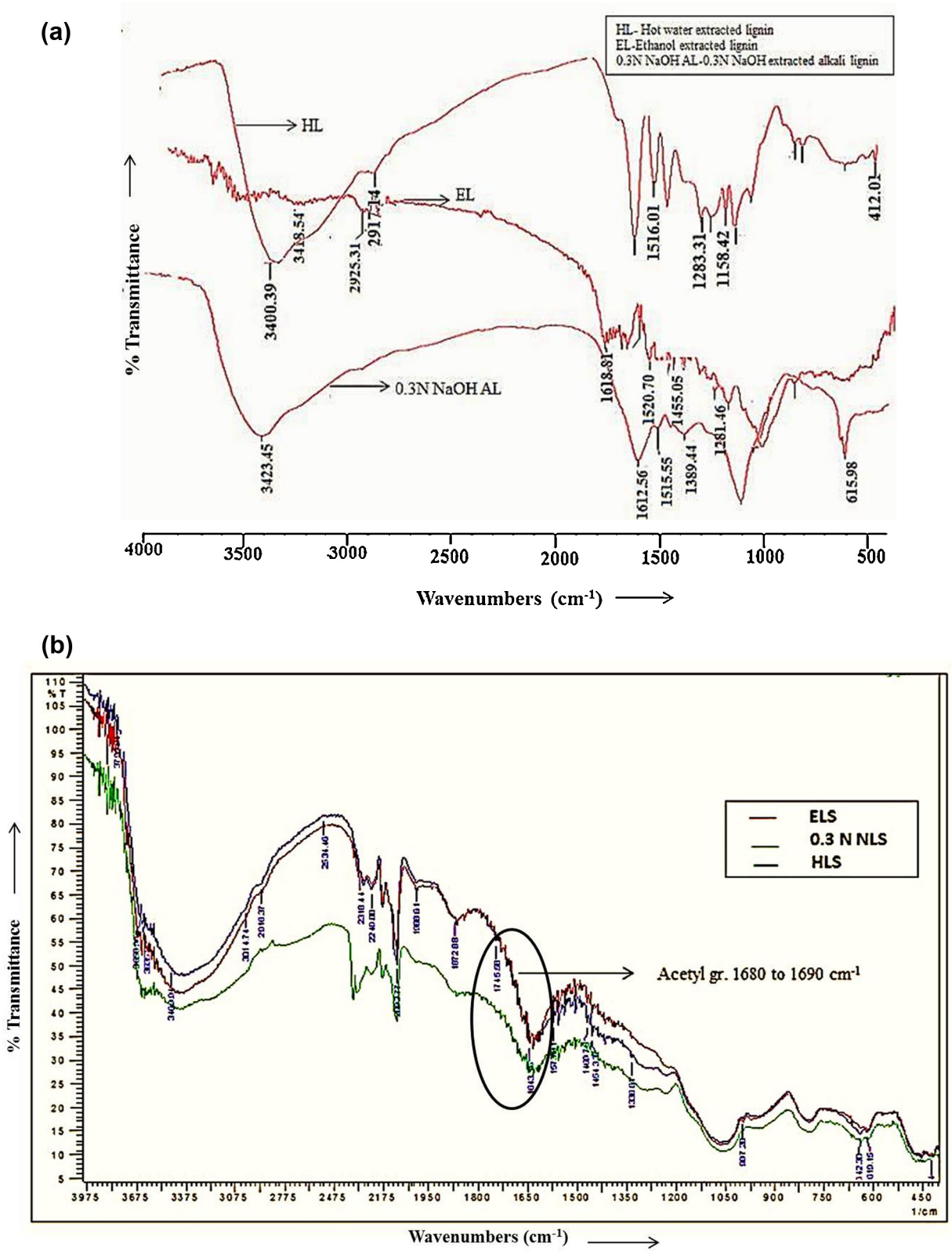

Fig. 2. (a) FTIR spectrum of RH extracted lignins (HL, EL and 0.3 N NaOH AL) and (b) FTIR spectrum of lignosilicate (LS) composites (ELS, 0.3 N NLS and HLS).

chemical structures of unmodified silica, lignin and lignin–silica hybrids. The major difference between the three spectra was the strong increase in the carbonyl stretching vibration (C=O) at 1680–1690 cm^{-1} after modification as shown in Fig. 2(b). In addition, the intensity of the band at 1250 cm^{-1} also increased and was associated to the C—O stretching vibration (C—O) of the acetate function. The intensity of the bands located at 2775, 1650, and 900 cm^{-1} in the spectrum of acetylated sample was enhanced. These bands were attributed to the C—H stretching (C—H), the C—H bending (C—H) and the C—H wagging (C—H) vibrations of

the methyl groups introduced, respectively [29]. The intensity of the band at 604 cm^{-1} also increased due to vibration of the methyl groups.

3.3.2. Particle size analysis

The particle size distribution (PSD) curves of the silica, HLS, ELS and 0.3 N NLS were determined by the standard test method [33]. The mean particle size (D_{50}) was found to be 1.341 μm, 12.86 nm, 18.98 nm and 14.89 nm for TEOS, HLS, ELS and 0.3 N NLS, respectively (Fig. 3). Nanocomposites are expected to provide benefits provided their size essential to maintain good dispersion is achieved. In the sol–gel method, TEOS is first hydrolyzed and combined with the functional groups of organic components (lignin). The particle size of LS is highly pH dependent. In our experiment, the pH of acidified lignin (pH 1.8) was raised to alkaline (pH 7.0) by addition of aqueous solution of TEOS. As the pH increased from acidic to alkaline range, condensed LS ionized and therefore became mutually repulsive resulting into nano-sized LS [34].

In the aqueous system the TEOS undergoes hydrolysis of alkoxy molecules followed by self-condensation reactions between the hydrolyzed silanes. The silane molecules are deposited on the silica surface through formation of siloxane bonds (Si—O—Si) between the silanol groups and hydrolyzed silanes with the release of water molecules leading to formation of particles having mean particle size in micron range [6].

3.3.3. Thermal properties (TGA–DTA)

The TGA curves for all silica–lignin composites in solid state showed no significant weight loss at temperature above 180 °C as shown in Fig. 4(1a), probably due to the subsequent absence/evaporation of water and volatile components from the hybrids. From 189 to 300 °C, the weight loss was nearly similar for all samples in relation to identical degradation processes of the acetylated lignin–silica. In the DTA curve of non-acetylated LS hybrids (controls) a weight loss of 0.014 mg min^{-1} and 0.027 mg min^{-1} was observed at 300.04 °C and at 693.56 °C (Fig. 4(1a–d)). The thermo gravimetric curves indicated a similar weight loss for HLS, ELS and 0.3 N NLS, which might be attributed to the similarity in the organization of chemical structure. A comparison of TGA–DTA measurements and the thermo grams for non-acetylated lignin–silica, acetylated HLS, ELS and 0.3 N NLS allowed us to conclude that acetylation of the lignin–TEOS affects the thermal stability of the material. The final degradation temperature of the lignin is increased when modified with acetylation reaction. The curves represent the decrease in the amount of oxidation during degradation, which, in turn, increases the thermal stability [26].

DSC is considered as an excellent technique for understanding the thermal behavior and identifying phase transitions such as glass transition, cold crystallization and melting temperatures of hybrids [31]. The results illustrated in Fig. 4(2) for ELS showed the highest T_g = 27.51 °C compared to HLS (T_g = 26.79 °C) and 0.3 N NLS (T_g = 27.05 °C). T_g of the hybrids was obtained at endothermic condition. In this study, the hybrid (0.3 N NLS) with lower T_g demonstrated highest melting temperature (T_m) at 337 °C with 727.34 J/mg enthalpy (Fig. 4(2b)) whereas that (ELS) having highest T_g (27.51 °C) showed lower T_m (179.99 °C) with 727.44 J/mg (Fig. 4(2c)). The significance of the highest glass transition of the 0.3 N NLS indicated that the acetylated lignin–silica hybrid was thermally the most stable and might be used as a raw material for the synthesis of various types of polymeric materials that required high temperature and thermal stability during applications. In HLS and 0.3 N NLS a large endothermic peak was followed by small exothermic peak (Figs. 4(2a and b)), whereas ELS showed a large constant exothermic peak followed by a small endothermic peak (Fig. 4(2c)) as reported earlier [26,30].

3.3.4. SEM analysis

The surface micrographs of LS composites obtained by SEM study presented at different magnification ranges demonstrated a remarkable lack of pores and cracks. Fig. 5a and b shows the SEM images of cross sections of untreated raw material (RH) whereas Fig. 5c and d shows chemically modified lignin, i.e., acetylated lignin having rough surface with small pores revealing the presence of silica particles embedded in the polymer network. Fig. 5e represents hot water extracted LS hybrid, showing dispersal of inorganic component on the surface of organic component. Fig. 5f and g represents 80% ethanol and 0.3 N NaOH extracted LS hybrids, respectively, characterized by a compact and dense structure of silica. Embedded silica particles could be clearly observed on the surface of lignin in both the micrographs. SEM analyses of hybrid revealed the formation of smaller aggregates assembled in porous networks. Due to the porous and rough surface of ELS, the capacity to adsorb metal ions is very high. The presence of a large number of small pores on the acetylated lignin surface enhanced the chances of lignin to incorporate silica because it promoted dispersion and penetration of the silica into the lignin.

3.3.5. Effect of the chemical structure of LS on metal bio-sorption

The maximum absorbance/bio-sorption of metal was obtained at 395 nm whereas several characteristic peaks were obtained due to the chemical reactions between hybrids and metal ions. Bio-sorption is mainly based on the presence of reactive groups that is related to the chemical structure of acetylated LS composites. However, certain surface components containing both hydrophilic and hydrophobic functional groups tend to migrate toward the surface of other components to make chemical bonds [26].

Binding of 0.1 M and 0.2 M of nickel to the surface of biosorbents were monitored and confirmed through FTIR spectroscopic analysis. Spectra representing the three LS bio sorbents (ELS, HLS, and 0.3 N NLS) were characterized by the presence of several characteristic peaks related to various functional groups of lignin, silica and metal ions (Fig. 6(1a and b, and 2a and d)) . The spectra obtained for metal incorporated LS catalysts are typical for hybrid materials with both components, organic and inorganic phases. The inorganic component was identified from the Si—O—Si modes observed below 1250 cm^{-1}, the typical silica bands at 1846 cm^{-1} and the silanol stretching bands above 3300 cm^{-1}. The weak band observed at 870 cm^{-1} for the entire catalysts might be attributed to

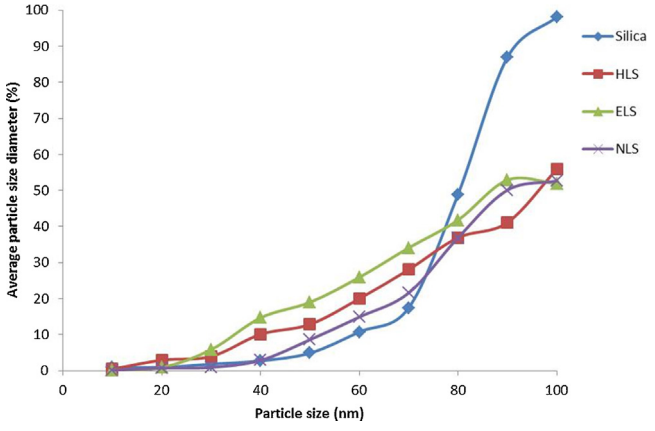

Fig. 3. Particle size distribution (PSD) graphs of LS composites at median range (D_{50}).

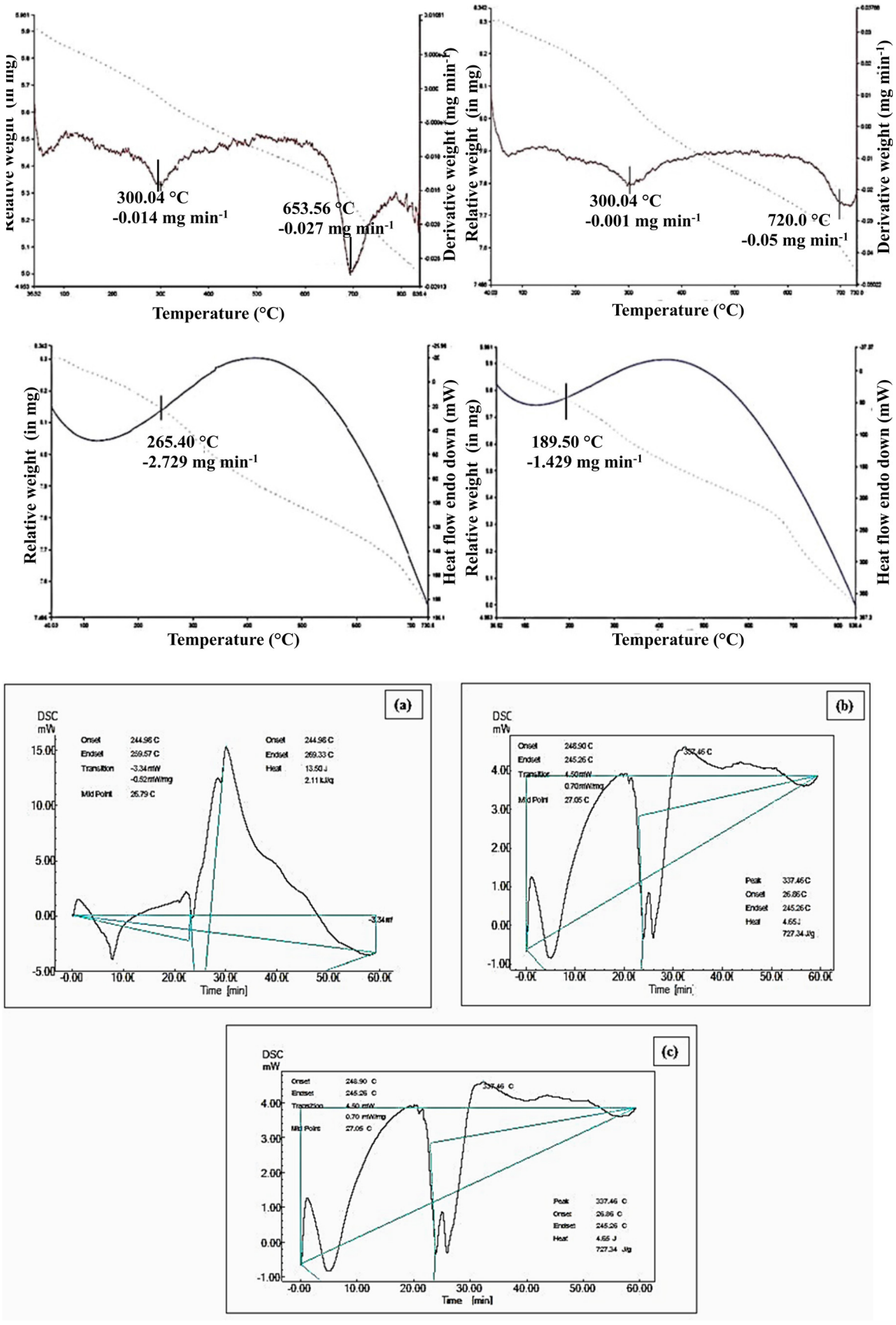

Fig. 4. (1) TGA–DTA analyses of (a) non-acetylated lignin–silica (control), (b) acetylated HLS, (c) acetylated ELS, (d) acetylated 0.3 N NLS. (2) Differential scanning calorimetric (DSC) analyses of lignosilicate composites (a) HLS, (b) 0.3 N NLS and (c) ELS

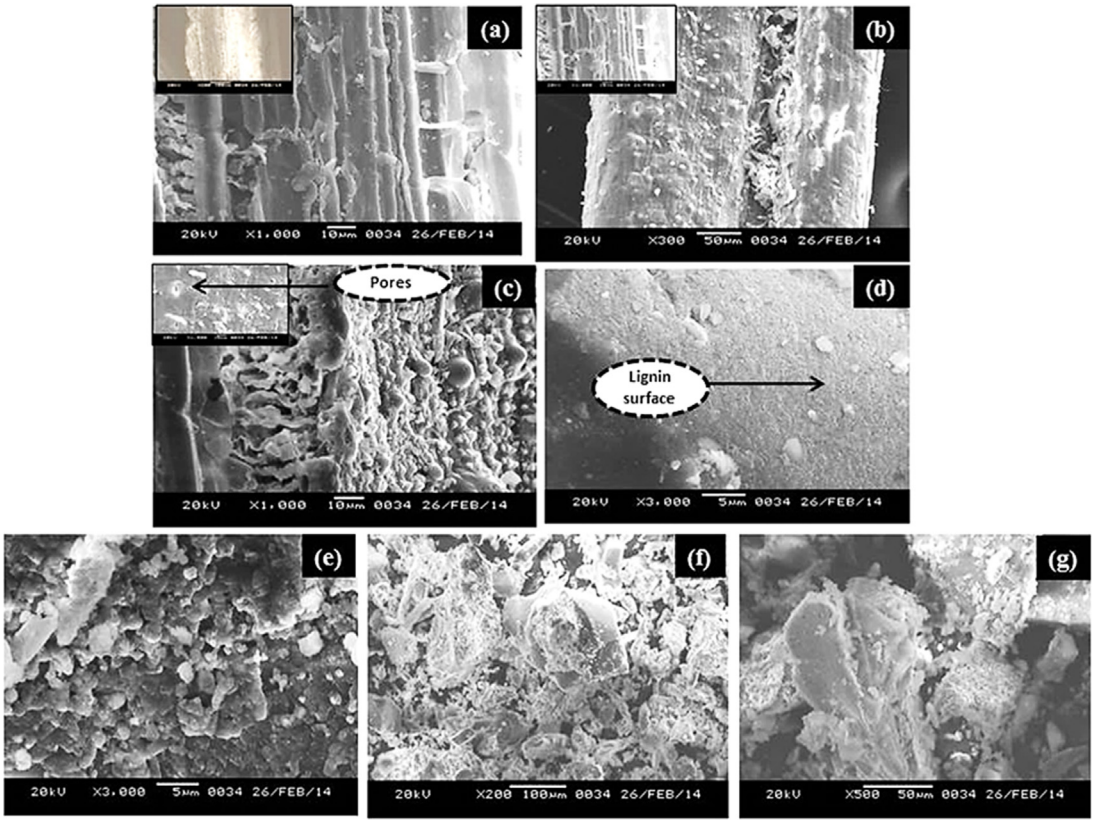

Fig. 5. Scanning electron micrographs (SEM) of lignin–TEOS hybrids (ligno-silicates). (a) and (b) RH raw material (untreated), (c) and (d) chemically modified lignin (acetylated lignin), treated showing micro pores on the surface of lignin molecule, (e) hot water extracted LS, (f) 80% ethanol extracted LS and (g) 0.3 N NaOH extracted LS.

Si—O—Ni^{2+}. The interaction between the carboxylate ion and the metal atom has been classified into four types: monodentate, bridging (bidentate), chelating (bidentate) and ionic interaction. It can be identified by the wave number separation (D) between IR bands [27].

The present study led us to conclude that the metal sorption capacity was more strongly influenced by the porous structure of the biosorbents rather than by the composition and quantity of dispersed superficial functional groups. Moreover, elution time was also found inversely proportional to the pore size of the composites as shown by 0.3 N NLS and the ELS, having smallest and largest pore sizes, respectively (Table 1). Finding suggested that the adsorption behaviour is dependent on the pore size and porous structure of LS composites as confirmed by PSD graph and SEM micrographs in Figs. 3 and 5(a–g), respectively.

3.3.6. Bio-sorption of nickel by LS composites

The effect of bio sorbent concentration on the bio-sorption process of Ni^{2+} is also considered as one of the most important factors. The variation in the molar concentration of biosorption of 0.1 M and 0.2 M of metal was studied at pH 6.0 as the optimum condition. The selected doses of hybrids were 0.1, 0.25, 0.5, 1.0, 1.5 and 2.0 g L^{-1}. The analysis was performed using AAS in two batches throughout the study. It is evident from the obtained data that the metal bio sorption values for Ni^{2+} at the two different molar concentrations are inversely proportional to the bio-sorbent dose and their elution times (Table 1). This could be possibly due to the larger pore size in HLS and the smaller in ELS for cationic metal ions at different concentrations as shown in Fig. 6(1a and b). The result directly supports the cation exchange mechanism. The order of selectivity with respect to the concentration range among the tested hybrids for 0.1 M and 0.2 M metal ions were observed as 0.3 N NLS > HLS > ELS. On the basis of the results of batch adsorption studies adsorption efficiency of hybrid for tested heavy metal ion was calculated (Table 1).

The removal efficiency by adsorption of 0.1 M metal solution as obtained by 0.3 N NLS (1.0 g L^{-1}), HLS (0.25 g L^{-1}), ELS (1.0 g L^{-1}), 0.3 N NLS (0.25 g L^{-1}), ELS (1.5 g L^{-1}) and HLS (0.892 g L^{-1}) showed 14.28% > 11.82% > 9.821% > 2.780% > 2.75% > 0.892% removal, respectively, whereas for 0.2 M metal ions as obtained by 0.3 N NLS (0.5 g L^{-1}), HLS (1.0 g L^{-1}), ELS (0.1 g L^{-1}), ELS (2.0 g L^{-1}), 0.3 N NLS (1.5 g L^{-1}) and HLS (0.1 g L^{-1}) showed 38.74% > 37.28% > 20.12% > 3.87% > 3.40% > 1.98% removal, respectively.

The findings clearly suggested that the most efficient biosorbent hybrid for metal ions was 0.3 N NLS as it showed the highest degree of rough surface. Differences in the metal sorption behaviour between the samples were thoroughly consistent with the surface characteristics of acetylated LS composites. Thus higher metal sorption ability for the 0.3 N NLS appears to be due to the greater content of —OH group present on the rough surface.

3.3.7. Mechanism and effect of pH on metal adsorption

Lignin is multifunctional phenolic polymer containing hydroxyl, carboxyl and carbonyl groups. Removal efficiency for metal ions increases after the organic substance has been modified to alter the surface charges and surface modification with the functional group acetate. Sol–gel reaction converts an aqueous metal alkoxide [Mn^{+} $(OR)_n$] solution into an inorganic network and molded gels which involves transformation of sol into gel. TEOS (alkoxysilane) have been used for the production of silica–gels. Mechanisms as well as the rates of both of the hydrolysis and condensation

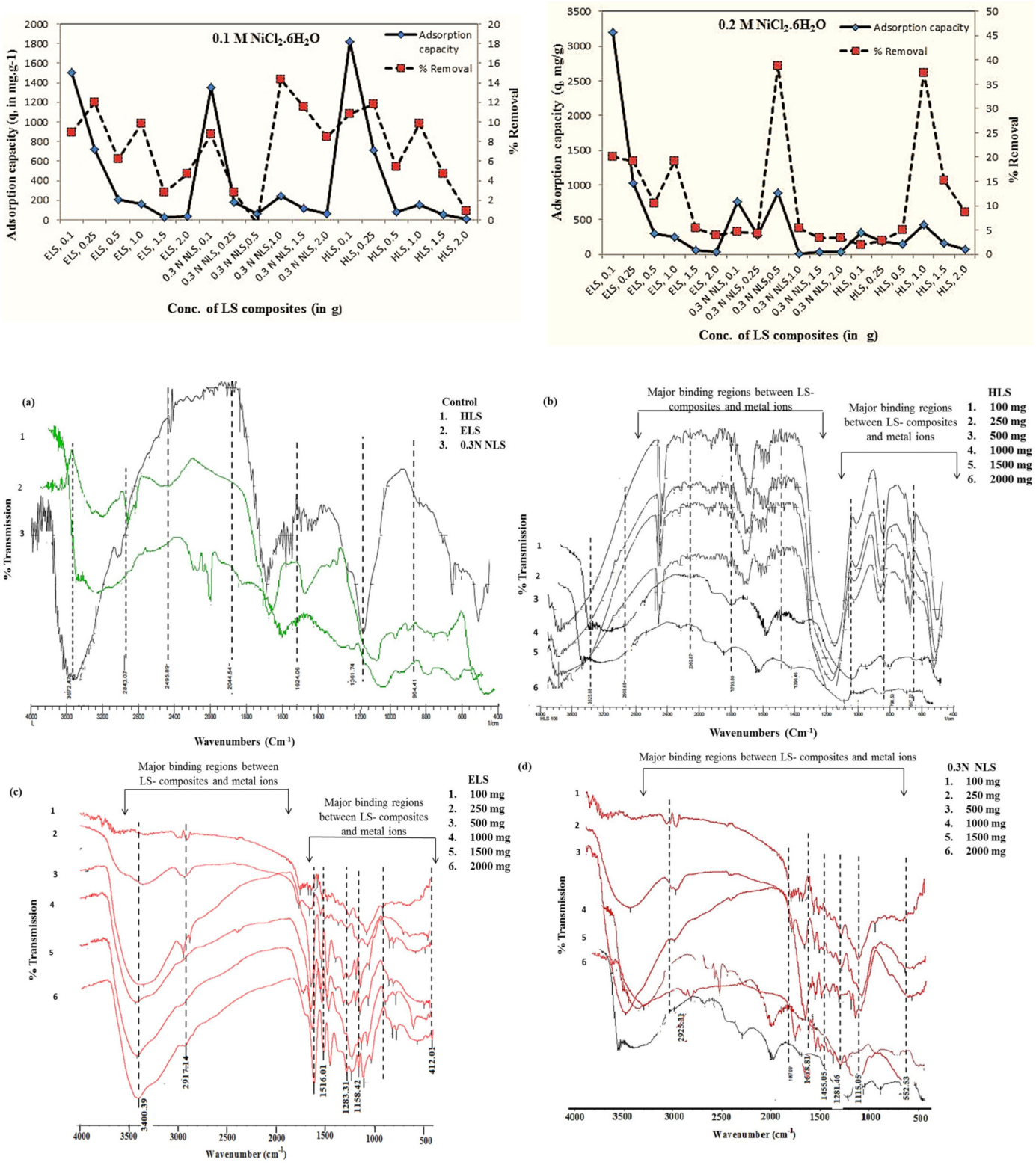

Fig. 6. (1) Effect of LS concentrations on adsorption capacity and percentage removal of (a) 0.1 M and (b) 0.2 M $NiCl_2{\cdot}6H_2O$. (2) FT-IR spectrum of metal bio-sorbents, (a) control, (b) HLS, (c) ELS and (d) 0.3 N NLS.

reactions depend strongly on the pH. TEOS having thiol groups on the composite surface showed high adsorption efficiency for metal ions [35]. To accomplish for such metal removal capacity, ion–ion interaction and binding of negatively charged LS composites to the positively charged metal ions on the surface of LS biosorbent at the acidic pH (6.0) range has been studied. The porous structure of lignins is not highly developed. However, the presence of significant amounts of different oxygen-containing groups in the

Table 1
Adsorption capacity (q) and removal efficiency (%) of lignosilicates (LS) for metal ions at different concentrations of the composites along with varying molar concentrations of $NiCl_2{\cdot}6H_2O$.

Serial no.	Sample concentration (in $g\,L^{-1}$)	Initial & final metal concentration (in ppm) of 0.1 M & 0.2 M $NiCl_2{\cdot}6H_2O$	Adsorption capacity (q) in $mg\,g^{-1}$ of the $NiCl_2{\cdot}6H_2O$ $q = \frac{(C_o - C_e)v}{w}$	Percent removal (in %) $\%R = \frac{(C_o - C_e)}{C_o} \times 100$
C_o of 0.1 M metal solution = 112			0.1 M $NiCl_2{\cdot}6H_2O$	
Final metal concentration in solution (C_e)				
1.	ELS, 0.1	102	1500	8.92
2.	ELS, 0.25	100	720	12
3.	ELS, 0.5	105	210	6.25
4.	ELS, 1.0	101	165	9.821
5.	ELS, 1.5	109	30	2.75
6.	ELS, 2.0	107	37.5	4.67
7.	0.3 N NLS, 0.1	103	1350	8.73
8.	0.3 N NLS, 0.25	108.97	181.8	2.780
9.	0.3 N NLS, 0.5	112.42	60	−0.37#
10.	0.3 N NLS, 1.0	96	240	14.28*
11.	0.3 N NLS, 1.5	100.45	115.5	11.49
12.	0.3 N NLS, 2.0	103.23	65.775	8.49
13.	HLS, 0.1	99.89	1816.5	10.81
14.	HLS, 0.25	100.16	710.4	11.82
15.	HLS, 0.5	106	180	5.357
16.	HLS, 1.0	102	150	9.80
17.	HLS, 1.5	107	50	4.67
18.	HLS, 2.0	111	7.5	0.892
C_o of 0.2 M metal solution = 106			0.2 M $NiCl_2{\cdot}6H_2O$	
Final metal concentration in solution (C_e) are as below				
1.	ELS, 0.1	84.67	3199.5	20.12
2.	ELS, 0.25	88.90	1026	19.23
3.	ELS, 0.5	96	300	10.41
4.	ELS, 1.0	89	255	19.10
5.	ELS, 1.5	100.23	57.7	5.44
6.	ELS, 2.0	101.89	30.825	3.87
7.	0.3 N NLS, 0.1	100.98	753	4.73
8.	0.3 N NLS, 0.25	101.39	276.6	4.34
9.	0.3 N NLS, 0.5	76.40	888	38.74*
10.	0.3 N NLS, 1.0	100.61	8.85	5.35
11.	0.3 N NLS, 1.5	102.39	36.1	3.40
12.	0.3 N NLS, 2.0	102.38	27.15	3.41
13.	HLS, 0.1	103.90	315	1.98#
14.	HLS, 0.25	103	180	2.83
15.	HLS, 0.5	101	150	4.95
16.	HLS, 1.0	77.23	431.55	37.28
17.	HLS, 1.5	89.90	161	15.18
18.	HLS, 2.0	96.89	68.325	8.59

Note: * Highest, # Lowest.

composite structure of lignin provides the polymer sorption activity. Mechanisms of the sorption include physical adsorption, hydrogen bonding, electrostatic interaction, and acidic–basic interaction. Strong electrostatic (i.e., ion dipole) interactions are expected to take place between the —OH ions of hydrolyzed silica and the electron-rich oxygen atoms [36].

At pH 6.0, the Ni^{2+} ions get precipitated due to hydroxide anions forming a nickel hydroxide precipitate. All samples indicated negative charge values favorable to the attraction between active sites of adsorbents and positive charges of metal ions, resulting in electrostatic interaction. Reactions between these two components may be due to the high pH of metal solution (6.0) than the value of isoelectric point (pI) of lignin (pI = 3.49) and TEOS (pI = 1.7–2.2) which may cause interaction between two charges (Fig. 7).

Depending upon the pH of the solution, presence of the LS composites in an aqueous solution caused the surface ion of lignin and TEOS to undergo protonation and deprotonation, after the chemical reactions during sol–gel process. An organic moiety (lignin) containing functional group that allows the attachment to an inorganic component (TEOS), can act as a surface modifier pH 6.0 causes an increase in the removal efficiency. This may be attributed due to the fact that at this pH range of the solution, the overall surface on the adsorbent became negatively charged and therefore, adsorption increased.

3.3.8. Statistical analyses

All the experiments were performed in triplicate. Data were statistically analysed by taking mean ± standard deviation to determine the yield of acetylated lignin and different types of LS composites using GraphPad prism 5.

4. Conclusion

The potential, availability and economics of using agrowastes far outweigh their limitations. An increasing population and constraints on using natural resources to grow fiber crops make agro-based fibers the most promising alternative to natural biofibers.

The present study demonstrates the suitability of rice husk extracted lignin as the substrate for synthesis of potential hybrid materials in combination with TEOS. Modification of the —OH groups of lignin by acetylation and synthesis of composite from acetylated lignin is important for the reaction parameters. The composite is thermally stable and its metal sorption capacity is strongly influenced by the porous structure of the bio-sorbents

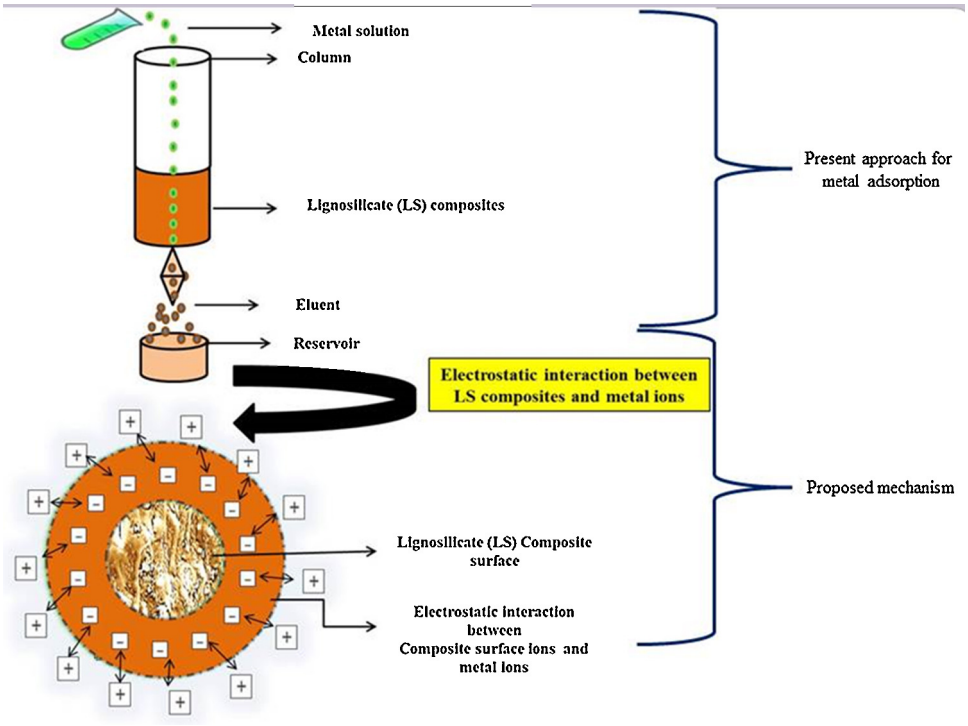

Fig. 7. Schematic diagram of column preparation and proposed mechanism of metal adsorption.

rather than the composition and quantity of dispersed superficial functional groups. Such ligno-silicate composite materials originating from rice husk may prove to be potential candidates to chelate or adsorb the environmental pollutants like heavy metal ions. Such attempts will increase the availability of co-products suitable for producing various chemicals thus reducing our dependence on non-renewable energy sources.

Future work will be focused on identification and characterization of potential mechanisms for removal of various environmental pollutants by producing LS based bio filters or bio membranes using biological component–TEOS based hybrids. Such hybrids can be utilized as economical biosorptive medium. Therefore, the future seems to be bright for agro-based and bio-based products.

Acknowledgements

Financial assistance in the form of DST-INSPIRE Senior Research Fellowship to one of us (KS) by the Department of Science & Technology (DST), Ministry of Science & Technology, Government of India is gratefully acknowledged. Authors wish to thankfully acknowledge the CGCOST, Raipur (C.G.) for FTIR analysis, STIC, Cochin (India) for TGA–DTA and to SAIF-NEHU, Shilong for SEM analysis.

References

[1] S. Barsberg, T. Elder, C. Felby, Lignin–quinone interactions implications for optical properties of lignin, Chem. Mater. 15 (3) (2003) 649–655.
[2] D. Ferdous, K. Dala, S.K. Bej, R.W. Thring, Pyrolysis of lignins: experimental and kinetics studies, Energy Fuels 16 (2002) 1405–1412.
[3] H. Arayik, M. Michael, D. Nicolas, F. Laurence, H. Anouck, C. Brigitte, A.B. Ve'ronique, Structure and optical properties of plant cell wall bio-inspired materials: cellulose–lignin multilayer nanocomposites, C. R. Biol. 334 (2011) 839–850.
[4] K. Sarita, K. Susheel, C. Annamaria, N. James, H. Youssef, K. Rajesh, Surface modification of inorganic nanoparticles for development of organic–inorganic nanocomposites—a review, Prog. Polym. Sci. 38 (2013) 1232–1261.
[5] M. Norgren, S. Notley, M. Majtnerova, G.A. Goran, Smooth model surfaces from lignin derivatives. I. Preparation and characterization, Langmuir 22 (2006) 1209–1214.
[6] H. Jun'ichi, S. Tetsuo, W. Yuuki, M. Katsuhiko, Preparation of silica–lignin xerogel, Langmuir 13 (1997) 4185–4186.
[7] B. Xiao, X.F. Sun, C.S. Run, The chemical modification of lignins with succinic anhydride in aqueous systems, Polym. Degrad. Stab. 71 (2001) 223–231.
[8] J.L. Atwood, J.M. Lehn, Comprehensive Supramolecular Chemistry, Pergamon Press, Oxford, 1996.
[9] N. Catherine, J. Ned, J. Silavwe, K. Kiptoo, E.R. Jonathan, Voltametric investigation of the distribution of hydroxo-, chloro-, EDTA and carbohydrate complexes of lead, chromium, zinc, cadmium and copper: potential application to metal speciation studies in brewery wastewater, Bull. Chem. Soc. Ethiop. 19 (1) (2005) 125–138.
[10] T. Jesionowski, L. Klapiszewski, G. Milczarek, Kraft lignin and silica as precursors of advanced composite materials and electroactive blends, J. Mater. Sci. 49 (2014) 1376–1385.
[11] T. Galina, D. Tatiana, J. Lilija, A. Anna, V. Alxander, P. Jevgenija, M.U. Nina, Synthesis of lignin-based inorganic/organic hybrid materials favourable for detoxification ecosystem components, BioResources 4 (4) (2009) 1276–1284.
[12] S. Nardis, D. Monti, C.D. Natale, A.D. Amico, P. Siciliano, A. Forleo, M. Epifani, A. Taurino, R. Rella, R. Paolesse, Preparation and characterization of cobalt porphyrin modified tin dioxide films for sensor applications, Sens. Actuators B 103 (2004) 339–343.
[13] K. Manabu, S. Hitomi, B. Bruno, M. Kimihiro, S. Yoshiyuki, Epoxy-based hybrids using TiO_2 nanoparticles prepared via a non-hydrolytic sol–gel route, Appl. Organomet. Chem. 27 (11) (2013) 673–677.
[14] M. Naushad, Organic and composite ion exchange materials and their applications, Ion Exch. Lett. 2 (2009) 1–14.
[15] Q.Y. Yumei, B. Tian, J. Zou, Y. Zhang, L. Zheng, L.Y. Wang, R. Chunguang, Z. Wang, A novel mesoporous lignin/silica hybrid from rice husk produced by a sol–gel method, Bioresour. Technol. 101 (2010) 8402–8405.
[16] I. Uzunova, S. Uzunovab, D. Angelovab, A. Gigova, Effects of the pyrolysis process on the oil sorption capacity of rice husk, J. Anal. Appl. Pyrol. 98 (2012) 166–176.
[17] Y. Guo, K. Yu, Z. Wang, H. Xu, Effects of activation conditions on preparation of porous carbon from rice husk, Carbon 41 (2003) 1645–1687.
[18] A. Farook, A.N. Jimmy, K. Zakia, T. Radhika, M.M.A. Nawi, Utilization of tin and titanium incorporated rice husk silica nanocomposite as photocatalyst and adsorbent for the removal of methylene blue in aqueous medium, Appl. Surf. Sci. 264 (2013) 718–726.
[19] M.B. Sciban, M.T. Klasnja, M.G. Antov, Study of the biosorption of different heavy metal ions onto Kraft lignin, Ecol. Eng. 37 (2011) 2092–2095.
[20] H. Jian, J. Yuxin, Z. Jianhong, Yu. Yuzhen, G. Zhang, Synthesis and characterization of red mud and rice husk ash-based geopolymer composites, Cem. Concr. Compos. 37 (2013) 108–118.
[21] H. Hengky, K.G. Karthikeyan, J.P. Xue, Copper and cadmium sorption onto kraft and organosolv lignins, Bioresour. Technol. 100 (2009) 6183–6619.

[22] M.A. Hashim, M. Soumyadeep, S.N. Jaya, S. Bhaskar, Remediation technologies for heavy metal contaminated groundwater, J. Environ. Manage. 92 (2011) 2355–2388.
[23] M. Borrega, K. Nieminen, H. Sixta, Effects of hot water extraction in a batch reactor on the delignification of Birch wood, Bioresour. Technol. 6 (2) (2011) 1890–1903.
[24] M. Altwaiq, S.J. Khouri, S. Al-luaibi, R. Lehmann, H. Drucker, C. Vogt, The role of extracted alkali lignin as corrosion inhibitor, J. Mater. Environ. Sci. 2 (3) (2011) 259–270.
[25] L.A.M. Nevarez, L.B. Casarrubias, A. Celzard, V. Fierro, V.T. Muñoz, A.C. Davila, J.R.T. Lubian, G.G. Sánchez, Biopolymer-based nanocomposites: effect of lignin acetylation in cellulose triacetate films, Sci. Technol. Adv. Mater. 12 (2011) 1–16.
[26] Y.K. Jae, H. Hyewon, O. Shinyoung, S.K. Yong, J.K. Ung, W.C. Joon, Investigation of structural modification and thermal characteristics of lignin after heat treatment, Int. J. Biol. Macromol. 66 (2014) 57–65.
[27] V. Uskokovic, Composites comprising cholesterol and carboxymethyl cellulose, Colloids Surf. B 61 (2008) 250–261.
[28] S. Olsson, E. Ostmark, R.E. Ibach, C.M. Clemons, K.B. Segerholm, F. Englund, The use of esterified lignin for synthesis of durable composites, in: E. Larnoy, G. Alfredsen (Eds.), Proceedings of the 7th Meeting of the Nordic-Baltic Network in Wood Material Science and Engineering (WSE), Oslo, Norway, October `27–28, 2011, pp. 173–178.
[29] L.M. Kline, D.G. Hayes, A.R. Womac, N. Labbe, Simplified determination of lignin content in hard and softwoods via UV-spectrophotometric analysis of biomass dissolved in ionic liquids, BioResources 5 (3) (2010) 1366–1383.
[30] L. Averous, F. Le Digabel, Properties of biocomposites based on lignocellulosic fillers, Carbohydr. Polym. 66 (2006) 480–493.
[31] A.U. Buranov, K.A. Ross, G. Mazza, Isolation and characterization of lignins extracted from flax shives using pressurized aqueous ethanol, Bioresour. Technol. 101 (2010) 7446–7745.
[32] S. Kubo, F.J. Kadla, Hydrogen bonding in lignin: a Fourier transform infrared model compound study, Biomacromolecues 6 (2005) 2815–2821.
[33] W. Stober, A. Fink, E. Bohn, Controlled growth of monodisperse silica spheres in the micron size range, J. Colloid Interface Sci. 26 (1968) 62–69.
[34] L.P. Singh, S.K. Agarwal, S.K. Bhattacharya, U. Sharma, S. Ahlawat, Preparation of silica nanoparticles and its beneficial role in cementitious material, Nanomater. Nanotechnol. 1 (2011) 44–51.
[35] E. Rosales, L. Ferreira, M.A. Sanroman, T. Tavares, M. Pazos, Enhanced selective metal adsorption on optimised agroforestry waste mixtures, Bioresour. Technol. 182 (2015) 41–49.
[36] T. Min, W. Jiali, M.D. Duncan, M.A. Robert, C. Aicheng, A novel approach for lignin modification and degradation, Electrochem. Commun. 12 (2010) 527–530.